

## WATER QUANTIFICATION FROM SPRAYER NOZZLE BY USING PARTICLE IMAGE VELOCIMETRY (PIV) VERSUS IMAGING PROCESSING TECHNIQUES

Muhammad Nadeem<sup>1</sup>, Young Ki Chang<sup>2</sup>, Uday Venkatadri<sup>1</sup>, Claver Diallo<sup>1</sup>, Peter Havard<sup>2</sup>  
and Tri Nguyen-Quang<sup>2,\*</sup>

<sup>1</sup>Department of Industrial Engineering, Dalhousie University, PO BOX 15000, Halifax, NS, B3H 4R2, Canada;

<sup>2</sup>Department of Engineering, Faculty of Agriculture, Dalhousie University, Truro, Nova Scotia, B2N 5E3, Canada

\*Corresponding author's e-mail: tri.nguyen-quang@dal.ca

Distribution of agro-chemicals through sprayer nozzles is very important because there is a significant loss of agro-chemicals such as pesticides during spraying due to non-uniformity of droplet and off-target drift. Improving the efficiency of spray pattern would reduce energy, costs and also minimize environmental pollution. In this paper, we examine jet patterns to study the performance of water distribution during the spraying process. We present a method to quantify water amount from a sprayer jet by using Particle Image Velocimetry (PIV) system in combination with imaging processing. For this study, ten sets of images were acquired with a PIV system in double frame mode. Each set of images contained different numbers of double-framed images: 10, 20, 30, 40, 50, 60, 70, 80, 90 and 100 at eight different pressures 25, 50, 75, 100, 125, 150, 175 and 200 kPa. The PIV images obtained were analysed using an image processing software for droplets and volume calculations. The results showed good agreement of both manual and PIV measurements and suggested that the PIV coupled with image processing technique can be used for a precise quantification of flow through sprayer nozzles.

**Keywords:** Image processing, PIV, spraying pattern, spray uniformity, volume quantification

### INTRODUCTION

Characteristics of the sprayer nozzles are important criteria in the application of different chemicals (pesticides, fungicides etc.) for different cropping systems, because of their direct effect on the efficiency of these chemical products. Previous research showed that uniform distribution of spray is very important, 30% of agricultural pesticide sprayed is lost during spraying due to the non-uniformity of droplet size and off-target drift (Bahrouni *et al.*, 2008; Miller and Ellis, 2000). The structure of the spray deposits can be affected by velocity, volume and size of the droplets (Guler *et al.*, 2007). Therefore, the study of the spray characteristics is very important for the ideal nozzle-velocity combination, which will optimize the spray efficiency with the appropriate dosage to the right targets (pests or insects on leaves etc.). In other words, parameters of spraying patterns such as the spray velocity, size of the droplet, volume distribution pattern, entrained air characteristics, structure of individual droplets, spray angle and spray structure play important roles for the efficiency of the agro-chemical application process (Miller and Ellis, 2000).

Our overall research goal is to examine the liquid jet properties during spraying processes to analyze the liquid distribution and uniformity of spraying patterns on plants with the objective of improving the sprayer nozzles design. This requires maximizing the uniformity of applied spray as a

function of operating pressures, nozzle parameters and wind effects. There are few papers in the literature dealing with this kind of issue except the works of Marcal and Cunha (2008) and Sudheer and Panda (2000).

Marcal and Cunha (2008) used water sensitive papers (WSP) coupled with image processing technique to observe the fraction of spray coverage, homogeneity parameters, stains and droplet numbers. The number of droplets per area was calculated using different scanning resolution and data was then compared with manually counted spots on WSP, but this method can measure the spray fraction coverage ranging from 7 to 50%. However, this method was not found to be suitable for more than 50% coverage on WSP due to submergence of droplets (droplets merging with each other).

Sudheer and Panda (2000) measured the droplet size produced by the sprinkler nozzles using image processing technique from Otsu (1979) to determine the threshold in image processing. The droplet size was also measured with the Pellet method (Sudheer and Panda, 2000) in a laboratory to compare the results of the images with actual results. This study revealed that droplet sizes less than 0.90 mm could not be measured in using the image processing technique but larger droplet sizes could be with more accuracy (Sudheer and Panda, 2000).

In this paper, we want to use the lab scale research in introducing the new imaging technique which is carried out through the acquisition of necessary information to support

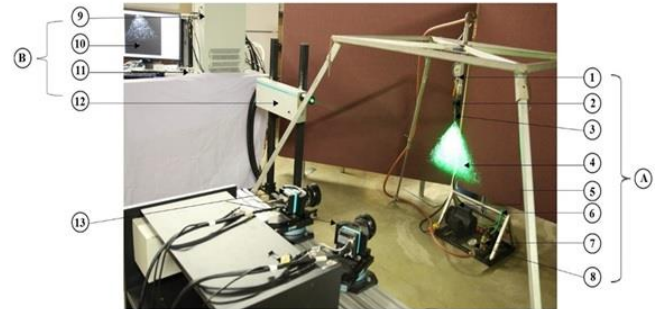
the development and implementation of an innovative sprayer nozzle. This will deal with different physical parameters of nozzle jets such as velocities, air-water flow properties, size of the droplet, volume distribution pattern, entrained air characteristics, structure of individual droplets, and spray structure. The PIV technique is used with the purpose of gaining more knowledge on jet behavior in determining relationships between velocity and pressure for sprayer system as well as to quantify the water from a sprayer jet. This technique is a non-intrusive laser optical measurement technique used to obtain instantaneous velocity vectors in a cross-section of gas or liquid flows. PIV can also be used for research and diagnostics into flow, turbulence, microfluidics, spray atomization and combustion processes (Adrian, 2005; Cao *et al.*, 2014; Hain *et al.*, 2007). Tracers (seeded particles) are used for submerged flow and airflow measurements (Grant, 1997; Husted *et al.*, 2009; Dabiri, 2009). Polyethylene tracers are commonly used. Tracer particles are added to the flow when flow is submerged while in case flow open to the air like nozzle flow in air the water droplets are considered as tracer particles. The particles are captured with high resolution camera and analysed for velocity or volume measurements (Hain *et al.*, 2007; Santiago *et al.*, 1998; Husted *et al.*, 2009). A key element in the PIV technique is the analysis of these images to measure the particles displacements and velocities. This method can measure an entire two-dimensional cross section of the flow field simultaneously. During the last decade, an increasing number of successful PIV applications have been reported such as indoor air flow measurements (Cao *et al.*, 2014), micro scale fluid flow (Angui *et al.*, 2010), liquid-liquid flow investigation (Morgan *et al.*, 2013) etc. The need to investigate different fluid flows requires that more theoretical studies be conducted to gain a deeper understanding of the PIV performance for data measurements.

Our main goal herein is therefore to use the PIV technique to examine the spray distribution and flow rate through sprayer nozzles as well as to obtain the quantity of water released from a sprayer by calculating the number of droplets passing through. The PIV images result was validated by experimentally measured water quantity from the sprayer nozzle. This technique brings a new water quantification technique in the context of research for sustainable irrigation.

## MATERIAL AND METHODS

The experiment was conducted in Biofluids and Biosystems Modelling Lab in the Department of Engineering, Faculty of Agriculture, Dalhousie University, Canada. Two parallel methods were used to measure the quantity of water going through sprayer nozzle manual measurement and PIV technique. A schematic diagram for a PIV system is shown in Figure 1. The standard PIV or Two-dimensional PIV system from LPU 550 (Dantec Dynamics, New York, USA) (Fig. 1)

was used to take the laser-illuminated images for the acquisition of the overall information of spray behavior (velocity of jet, spray spread and images for the number of droplets calculation).



A= Prototype of spray nozzles B= Operational components of PIV 1. Pressure gauge, 2. Flow control valve 3. Nozzle assembly 4. Spray sheet with laser 5. Electric motor, 6. Suction and by pass pipe 7. Pressure control valve, 8. Pressure gauge 9. Synchronizer 10. Computer, 11. Laser controller 12. YLF laser 13. CCD cameras.

**Figure 1. PIV system and prototype of sprayer nozzle.**

**Image acquisition by PIV:** The spray sheet was illuminated by the beams of diode-pumped Nd:YLF laser (dual-cavity, pulsed laser 135-15 Dantec Dynamics, New York, USA), with pulse energies up to 30 mJ and repetition rates of up to 10 kHz. For imaging of the spray sheet a Flow Sense EO CCD camera (Flow Sense EO 11M 9080X6231, Dantec Dynamics, New York, USA) with 6.5 frames per second at full resolution at sensor resolution 4008 x 2672 pixels, inter-frame time 300ns and pixel size 9µm was used. The CCD camera was aligned at an angle of 90° to laser beam and it was focused on the laser and spray sheet. The liquid spray sheet was produced using an extended range flat fan sprayer nozzle (TeeJet 8003) and an electric pump of 0.4 hp (298.27 W). For the manual measurement, a glass cylinder of 110.424 L (91.44cm x 30.48cm x 39.62cm) was used to collect and provide the liquid to the pump for continuous spray sheet. The sprayer nozzle was equipped with electric pump, pressure gauges, control valves and by pass pipe (Fig. 1).

**Droplets calculation:** The number of droplets appearing within the double framed images for each laser sheet were measured using the ASABE S572 (American Society of Agricultural and Biological Engineers, 2010). According to this standard, the diameter of one droplet for the specific nozzle TEEJET 8003 (extended range flat fan) used in the study is 288 µm (0.288 mm). The average volume of one droplet can be calculated by the following formula:

$$V_{\text{drop}} = \left(\frac{4}{3}\right) \pi r^3 = \left(\frac{4}{3}\right) \pi (0.144)^3 = 0.012507 \text{ mm}^3 \quad (1)$$

and the total number of droplets  $N_1$  is hence given by:

$$N_1 = V_{\text{water}} / V_{\text{drop}} \quad (2)$$

Where:  $V_{\text{drop}}$ : Average volume of one droplet ( $\text{mm}^3$ )

$V_{\text{water}}$ : Real total volume of water released from the spray nozzle (manually measured) ( $\text{mm}^3$ )

$N_1$  : Total number of droplets released from sprayer (calculated manually).

**White pixels determination:** A computer processing program (custom-made) was designed and implemented in C++ combined with Visual Studio 2010 (Microsoft®, Redmond, WA, USA). This program was used for image processing of spray sheet obtained through PIV, including segmentation with different thresholds and counting of white pixels of segmented images as well as Otsu's threshold method previously mentioned Otsu (1979). The Otsu's method could not in fact provide an appropriate threshold in this study as experimental images did not have bimodal distribution and contained lots of various intensity pixels due to different reflected angles. Then, the threshold values from 0 to 254 were compared to find the highest value of coefficient of determination ( $R^2$ ) between manually measured volume and the number of white pixels after segmentation (Fig. 2). A threshold value ( $> 0$ ) (Fig.3-c) showed the highest  $R^2$  value. Moreover, the brightness of pixels was caused by an incident

angle, so the threshold value ( $> 0$ ) was a more reasonable choice.

The total number of white pixels ( $N_2$ ) was calculated by using above mentioned custom built image processing program in the laser sheet images. The program identified adjacent regions of uniform white-scale levels. This program was also used to identify all the individual droplets in the image as well as other noise-type items such as the spray nozzle and the pump close to the spray nozzle. The algorithm requires that the 256-level gray scale (8-bit gray scale) images acquired by the PIV camera to be dithered to a black and white image. This was accomplished by choosing a "Threshold" value above all values were white and below or equal to which all were black. There is typically a range of about 60 grey-scale levels out of 256 where the number of drops identified is invariant. The threshold was set within this invariant region. From a pair of two PIV images, only the second image was used to avoid double counting of white pixels. In the meantime, manual measurement of the spraying liquid was

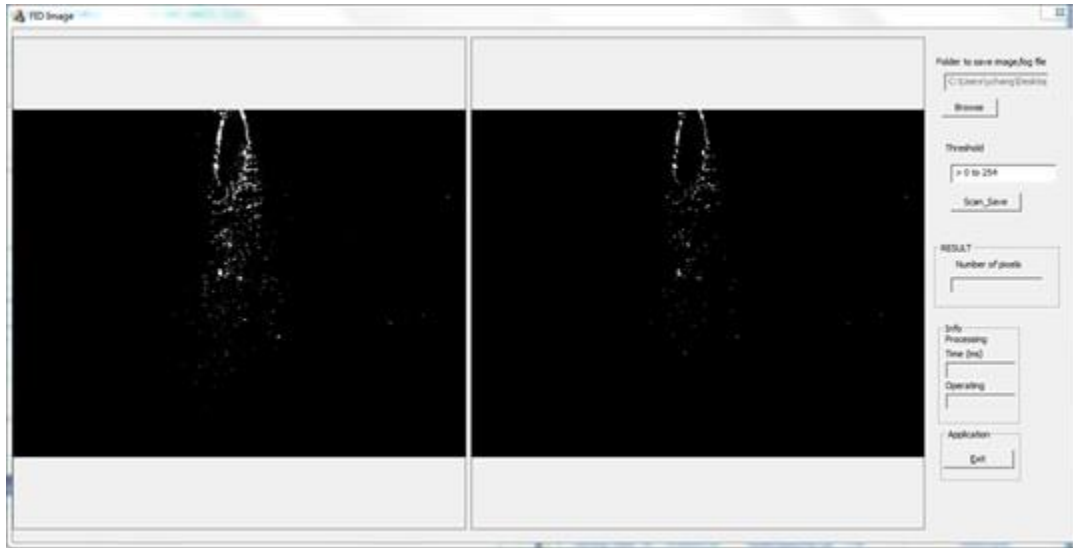


Figure 2. Image processing program that segments a PIV image to black/white image using different threshold values (0 to 254).

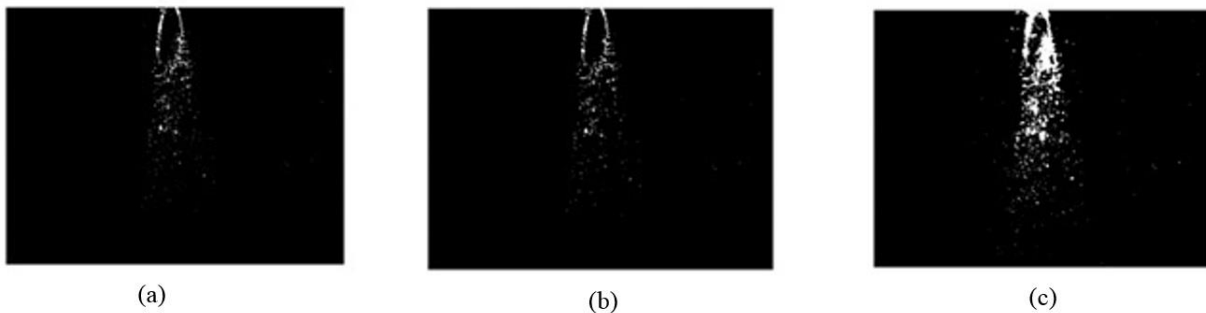
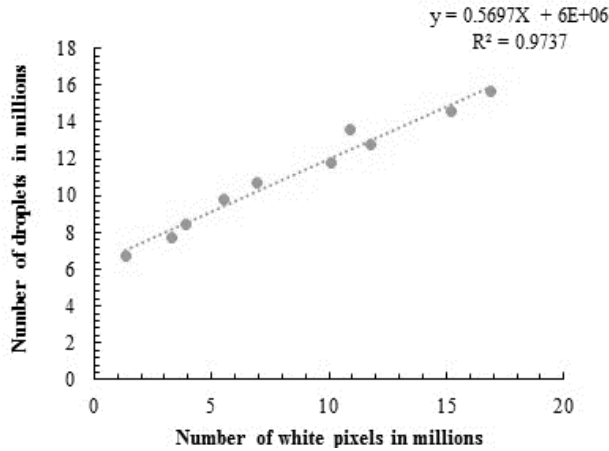


Figure 3. (a) Original image (b) Otsu threshold image (c) Threshold ( $>0$ ).

also made. A plastic pan was used as a drop collector to measure the liquid spray volume released, equivalent to each set of images by using the same PIV system settings.

**Volume and absolute error calculation:** The next step was to find the relationship between droplet size and number of white pixels, for that 8 graphs were plotted between numbers of white pixels and numbers of droplets (calculated by using equation 1 and 2) at different pressures.



**Figure 4. Relationship between white pixels and number of droplets at 25 kPa pressure**

We used linear regression among the number of white pixels and the number of droplets calculated by manual method. For example, at 25kPa (Fig. 4), the regression equation indicated that one pixel from the PIV image is equivalent to  $0.5697X + 6 \times 10^6$  droplets.

$$N_3 = (0.5697 \times N_2 + 6 \times 10^6) \quad (3)$$

$N_2$  = Number of white pixels in a PIV double frame images

$N_3$  = Total number of droplets released from the sprayer in a fixed time.

This equation (3) was used to determine the number of droplets (based on white pixel)  $N_3$ .

Finally, to calculate the measured volume of the water going through, we applied the following formula (4).

$$V_{\text{PIV-water}} = N_3 \times V_{\text{drop}} \quad (4)$$

Equation (5) was used to find out the percentage absolute error between the two volumes of water, one determined by PIV and the other one manually measured:

$$\text{Error} = |(V_{\text{PIV-water}} - V_{\text{water}}) / V_{\text{water}}| \times 100 (\%) \quad (5)$$

In the same manner of Figure 4, relationships between number of white pixels and number of droplets were graphed at different pressures (50, 75, 100, 125, 150, 175 and 200 kPa) and their regression equations for this duo pixel-droplet are presented in Table 1.

**Statistical analysis:** To find out the best combination of pressure and number of pictures at which least significant error would be achieved the factorial analysis was carried out followed by the multiple mean comparison by using LS mean

at  $p \leq 0.05$  level of significance. The statistical analysis of the data was performed using Minitab 17 (Minitab Inc., Pennsylvania, USA).

**Table 1. Regression equations and  $R^2$  obtained from graphs at different pressures**

Pressure (kPa)	Regression equation	$R^2$
50	$N_3 = 0.6218 N_2 + 8E+06$	0.9907
75	$N_3 = 0.5755 N_2 + 9E+06$	0.9952
100	$N_3 = 1.2132 N_2 + 9E+06$	0.9877
125	$N_3 = 1.1160 N_2 + 1E+07$	0.9837
150	$N_3 = 1.0021 N_2 + 1E+07$	0.9807
175	$N_3 = 1.0826 N_2 + 1E+07$	0.9652
200	$N_3 = 1.0375 N_2 + 1E+07$	0.9729

Where:  $N_2$  = Number of white pixel and  $N_3$  = Number of droplets measured through white pixels.

## RESULTS AND DISCUSSION

**Image acquisition by PIV:** The spray sheet of the extended range flat fan sprayer nozzle was illuminated by pulsed laser sheet at eight different pressures (25, 50, 75, 100, 125, 150, 175 and 200 kPa) shown in Figure 5. Ten sets of images were acquired using the above-described PIV system setting, with a double frame mode at a trigger rate of 4 Hz, and time between pulsed signals of 500  $\mu$ s. Each set of images contained the different number of double frame images: 10, 20, 30, 40, 50, 60, 70, 80, 90 and 100. This procedure was replicated three times to reduce the biasness in data. The data was processed by using Dynamic Studio v4.00 software (Dantec Dynamics, New York, USA), which contains tools for configuration, acquisition, analysis and for post-processing of the acquired data.

**Uniformity of velocity distribution in the spray particles:**

The acquired images from PIV were analyzed to find out the velocity of spray particles at different positions (both vertical and horizontal). The adaptive PIV method was used to calculate the velocity vectors. This method adjusts the size and shape of interrogation areas (IA) to adapt to local seeding densities and flow gradient. The velocity information of spray sheet then was exported as numeric data for graphical representation.

To verify the uniformity of velocity distribution, we used the standard classical notion of normal distribution. All velocity data measured by PIV were exported and treated statistically, i.e., the mean and standard deviation for velocity data at different points under the spray nozzle were calculated. If the velocity distribution follows the normal distribution pattern, it shows that there will be a uniformity distribution of spray sheet.

We used the velocity vectors at four different positions (10, 20, 50 and 70 mm) under the tip of nozzle determined from the PIV images to verify the velocity distribution. All velocity data were reported in the graphic versus their frequency

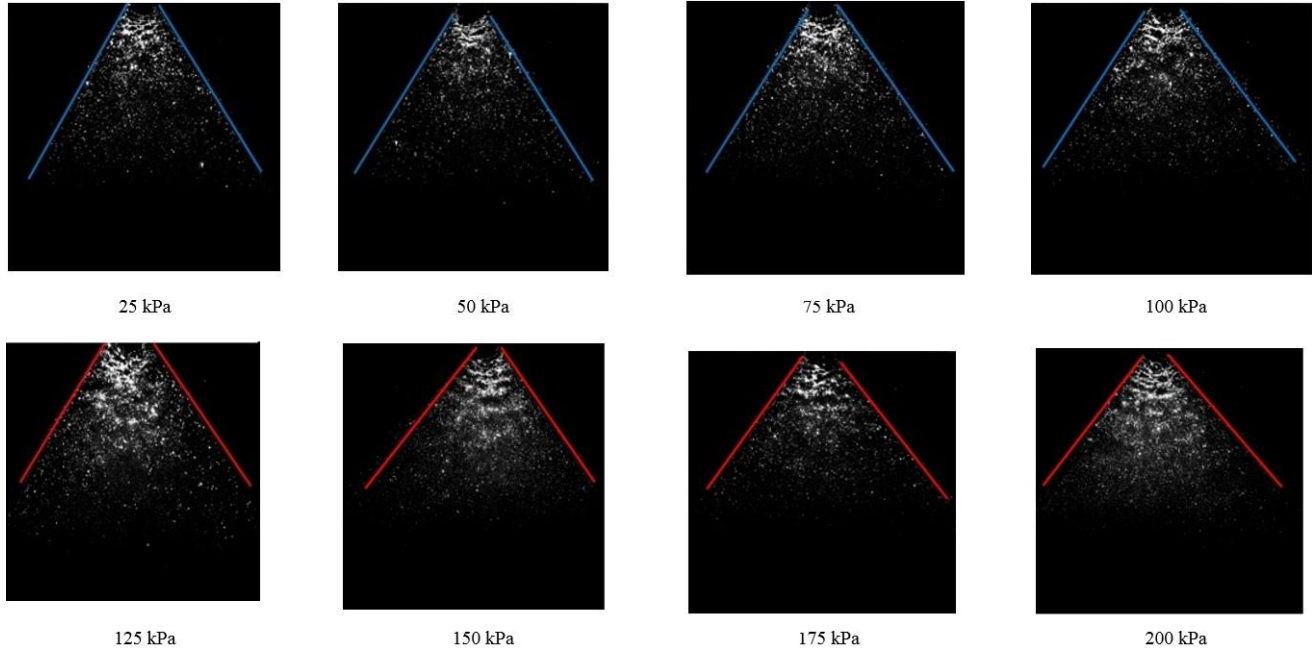


**Figure 5. PIV Images acquired for analysis at different pressures.**

(Fig. 6) showing that the velocity distribution follows the normal distribution equation with a mean value of 8.84 and median of 9.5. We can see that the mean value and median were not very different, in other words, the mean value is close to the median value.

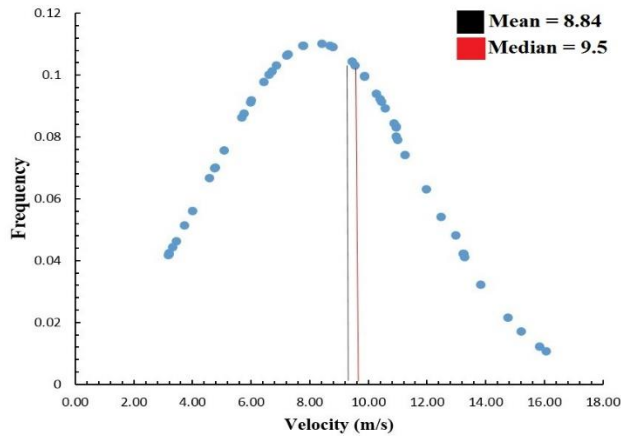


**Figure 6. Velocity distribution under the sprayer nozzle at 200 kPa pressure.**

It demonstrated that the spraying water particles were uniformly distributed, i.e., there was a uniformity of spraying water around the symmetrical axis of the sprayer nozzle. In an ideal scenario, the mean value had to be the median of this distribution, which means the velocity distribution is in perfect uniform. However, due to the asymmetrical laser source (the laser beam just coming from one side), we cannot

have a perfect and symmetrical enlightening situation for each PIV image, our graph in Figure 6 hence cannot reach the perfect normal distribution.

Figure 7a,b,c,d showed the velocity profiles at 10 mm, 20mm, 50mm and 70mm distances under the sprayer nozzle. From these profiles, we can see that the velocity has the maximum value at the centre of nozzle (outlet of the flow) and the velocity field is uniformly distributed on each left and right side, but not totally perfect.

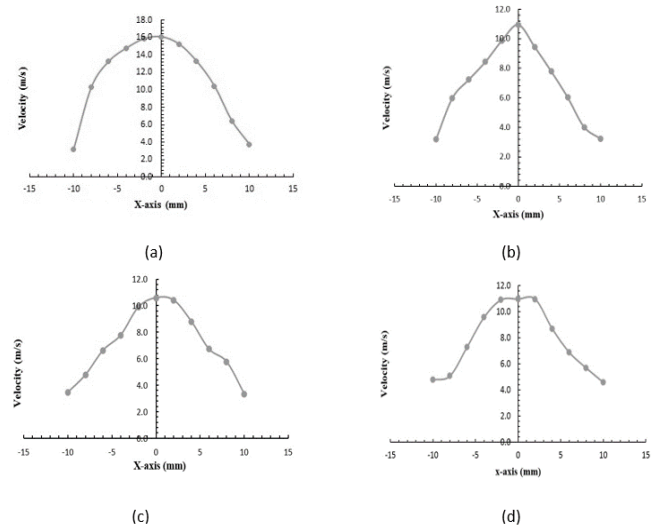


**Figure 7. Velocity distribution profiles under the sprayer nozzle at 10 mm (a), 20 mm (b), 50 mm (c) and 70 mm (d) distance at 200 kPa pressure.**

**Manual measurements for water volume versus PIV results:**

After validating the normal distribution of the spray sheets, these PIV images were used to calculate the volume of spray sheet. Volume of one drop of spray coming out of the sprayer nozzle was calculated using equation (1) while the number of droplets ( $N_1$ ) was calculated by dividing the volume of water manually collected and average droplet volume at the lowest pressure 25 kPa (Table 2). The calculations for the total number of droplets ( $N_3$ ) was done by using the data from regression equations presented in Table 1. To calculate the

volume of water from PIV Equation (4) was used while Equation (5) was used to calculate the percentage absolute error. These calculations were also done for other pressure ranges including 50, 75, 100, 125, 150, 175 and 200 kPa (all are presented in Table 3).

It is noted that the manually measured volume and the PIV based volume, compared in Table 3, are very close to each other (relative error less than 5%) when the number of double-framed pictures at 10, 60, 70, 90 and 100, captured under the 25kPa pressure (Table 2). Under that pressure, the error is

**Table 2. Calculated spray volume using PIV and manually measured methods at 25 kPa pressure**

No. of pictures	$N_2$	$N_3$	$V_{PIV-water}(mL) = N_3 \times V_{drop}$	$V_{water}(mL) = N_1 \times V_{drop}$	% E
10	1357707	6773485.678	84.7159854	84.33	0.453737597
20	3324186	7893788.764	98.7276161	96.33	2.485414610
30	3899246	8221400.446	102.8250554	106.00	2.995230773
40	5546436	9159804.589	114.5616760	120.67	5.062007129
50	6922519	9943759.074	124.3665947	130.00	4.333388660
60	10096836	11752167.470	146.9843585	147.00	0.010640451
70	11772475	12706779.010	158.9236850	159.33	0.257101435
80	10920085	12221172.420	152.8502035	160.33	4.667232736
90	15192179	14654984.380	183.2898896	182.33	0.524619522
100	16875515	15613980.900	195.2840591	196.00	0.365275990

Where:  $N_1$  : Total number of droplets released from sprayer,  $N_2$  = Number of white pixel,  $N_3$  = Number of droplets measured through white pixels,  $V_{PIV-water}$  = Predicted volume= Volume measured by using PIV (mL),  $V_{water}$  = Manually measured volume (mL),  $V_{drop}$  : Average volume of one droplet and E = % Absolute Error.

**Table 3. Calculated spray volume using PIV and manually measured methods at different pressures**

No. of Pictures	25 kPa			50 kPa			75 kPa			100 kPa		
	$V_1$	$V_2$	% E	$V_1$	$V_2$	% E	$V_1$	$V_2$	% E	$V_1$	$V_2$	% E
10	84.72	84.33	0.4537	114.9	108.0	6.403	128.00	132.33	3.277	134.33	140.67	4.507
20	98.73	96.33	2.4854	129.8	132.7	2.185	145.73	146.00	0.182	155.78	163.33	4.623
30	102.83	106.00	2.9952	144.5	139.7	3.472	162.38	158.00	2.775	176.86	188.33	6.091
40	114.56	122.67	5.0620	159.9	153.0	4.515	179.07	179.33	0.149	199.35	206.33	3.386
50	124.37	134.00	4.3334	172.4	164.0	5.128	196.33	193.67	1.375	224.35	228.33	1.747
60	146.98	147.00	0.0106	186.5	184.0	1.361	213.80	209.00	2.297	262.41	250.00	4.966
70	158.92	159.33	0.2571	202.3	194.0	4.253	229.40	231.00	0.691	267.12	267.33	0.078
80	152.85	169.67	4.6672	216.6	207.3	4.481	246.73	253.33	2.607	288.88	294.67	1.965
90	183.29	182.33	0.5246	228.8	230.0	0.516	268.15	268.67	0.192	309.87	324.67	4.559
100	195.28	196.00	0.3653	243.0	240.0	1.268	284.33	282.33	0.706	333.98	345.33	3.288
No. of Pictures	125 kPa			150 kPa			175 kPa			200 kPa		
	$V_1$	$V_2$	% E	$V_1$	$V_2$	% E	$V_1$	$V_2$	% E	$V_1$	$V_2$	% E
10	145.18	157.33	7.726	150.23	155.33	3.283	156.48	175.67	10.92	154.00	198.33	22.35
20	165.47	188.67	12.297	174.81	184.00	4.993	186.13	193.00	3.56	183.45	227.33	19.30
30	186.36	195.67	4.757	200.41	207.67	3.493	206.42	222.33	7.16	213.42	230.67	7.48
40	207.32	246.00	6.328	225.03	235.33	4.377	230.91	251.67	8.25	242.66	275.67	11.97
50	228.79	254.67	4.937	249.94	254.00	1.600	257.70	273.33	5.72	271.01	283.67	5.68
60	249.94	271.67	7.998	276.29	311.33	11.255	291.26	263.00	10.75	302.49	309.33	2.21
70	271.27	292.33	7.205	302.89	328.33	7.750	322.05	322.67	0.19	328.94	346.00	4.93
80	292.53	310.00	5.634	328.49	335.00	1.944	346.43	364.33	4.92	366.74	401.00	8.54
90	311.53	326.67	4.633	353.00	358.67	1.581	376.25	406.00	7.33	388.42	421.00	7.74
100	333.41	353.67	5.728	379.79	379.67	5.446	403.52	416.00	3.00	415.76	465.67	10.72

Where:  $V_1$  = volume of water measures through PIV and image processing technique in mL,  $V_2$  = Manually measured volume in mL and % E = % Absolute Error

**Table 4. Analysis of variance**

Source	DF	MS	F-Value	P-Value
Pressure	7	184.44	16.44	<0.001
No. of Pictures	9	60.95	5.43	<0.001
Pressure x No. of Pictures	63	26.37	2.35	<0.001
% Absolute Error	160	11.22		
Total	239			

DF = degree of freedom MS = mean square

**Table 5. Two-way interaction effect (pressure × number of pictures) of important interactions**

Pressure (kPa)	No. of pictures	Mean % absolute error)	Pressure (kPa)	No. of pictures	Mean (% absolute error)
200	10	22.22 a	25	100	0.9754 de
200	20	19.27 ab	25	90	0.9749 de
175	60	144.94 abc	75	40	0.5454 de
200	40	11.98 a-d	75	90	0.2657 de
125	20	11.73 a-e	175	70	0.2110 e

Means with same grouping letter are not significantly different at the 5% level using LS mean

very significant (greater than 5%) when the number of pictures was at 40. We notice a question arising herein is what combination of number of pictures and operational pressure could give the least significant error with the well-defined PIV configuration. The answer to that question is obtained by the following factorial analysis where the pressure and number of pictures were considered as two input factors while the error was considered as output.

**ANOVA (analysis of variance) and multiple means comparison (MMC) tests:** From Table 3, it is difficult to identify the pair of pressure and number of pictures which provide the least percentage absolute error. To answer this question the factorial analysis was carried out by considering pressure and number of pictures as factors and % absolute error as response variable. The Table 4 shows the ANOVA results indicating the effects of pressure and number of pictures on percent absolute error. Based on these results, two-way interactions (pressure x No. of Pictures) and main effect of pressure and number of pictures were found to be significant. These results suggested MMC of two-way significant interaction effect.

The results of ANOVA suggested MMC of the significant interaction effects, indicated by Table 4. As the experiment was done in lab, therefore the magnitude of error is expected to be from moderate to high suggesting therefore, LS means was used as the method for MMC only for two-way interaction.

The MMC results of important interactions are shown in Table 5. The non-relevant interactions are not presented here. These results showed that maximum percent absolute error (22.220) was obtained when pressure = 200 kPa and number of pictures = 10. The percent absolute error obtained when the factors interacted at this level was significantly different (higher) from the percent absolute error obtained at all other

combinations, except for pressure = 200 kPa and number of pictures = 10.

Moreover, the results indicated that minimum error was obtained when pressure and number of pictures interacted at pressure = 175 kPa and number of pictures = 70. The mean percent absolute error obtained when the factors interacted at this level was significantly different (lower) from the mean percent absolute error obtained at all other combinations, except for pressure = 175 kPa and number of pictures = 70 significantly less error.

Also, the less perfection of the PIV system when dealing with the more turbulent flow. For 10 pictures set and 200 kPa pressure the highest *percent* absolute error (22.220%) was observed possibly due to the accuracy of correlations and the short period of measurement time. The least error (0.2110%) was found with 70 pictures set with 175 kPa pressure, and it seemed being an optimal number of pictures for correlation and our pattern recognition processes. It is noticed that results from different statistical analyses have shown a good agreement of both these measurements, this suggests that the quantification of flow through sprayer nozzles by the PIV technique coupled with image processing could be reliable and accurate.

**Conclusions:** The PIV technique coupled with image processing could be used for a precise quantification of flow streams through sprayer nozzles as well as for the velocity distribution of spraying pattern. Our results showed that the velocity reaches the maximum value at the center of nozzle and becomes less powerful at the left and right sides within the spraying pattern. The field of velocity also showed a uniform and asymmetrical distribution on the entire area of spraying.



The results of this research reveal that fluid flow measurement through PIV is a reliable and can predict the spray pattern accurately. The methodology of this research can be used for quantification of water coming out of sprayer nozzles used in precision irrigation (drip irrigation, sprinkler irrigation etc.). It would open a new horizon in the future for the use of PIV technique to investigate the characteristics of sprayer nozzles air-water flow properties, submerged flow, internal geometry of the spray, performance as well as flow rate through a sprayer nozzle. Future research works will investigate the impact of volume flow rate and spray angles on the uniformity of spray distribution and droplet size. This would require the design of a new experimental set up to control spray angle and flow rate.

Our expected outcome is to reduce the time and labor and hence cost investment for the spraying in crop productions in applying a sophisticated method such as PIV.

**Acknowledgements:** This work was supported by the Canada Foundation for Innovation (CFI) Grant No 31188, Nova Scotia Research and Innovation Trust (NSRIT) and Natural Sciences and Engineering Research Council of Canada (NSERC) Grant No 34119 of TNQ. MN wants to acknowledge the support from University of Agriculture Faisalabad (Pakistan).

## REFERENCES

- Adrian, R.J. 2005. Twenty years of particle image velocimetry. *Exp. Fluids* 39:59-169.
- Angui, L., E. Qin, B. Xin, G. Wang and J. Wang. 2010. Experimental analysis on the air distribution of powerhouse of Hohhot hydropower station with 2D-PIV. *Energ. Convers. Manage.* 51:33-41.
- American Society of Agricultural and Biological Engineers. 2010. Spray nozzle classification by droplet spectra. Standard Technical Note - S572 Chart. ASABE, Saint Joseph, Missouri, United States of America.
- Bahrouni, H., C. Sinfort and E. Hamza. 2008. Evaluation of pesticide losses during cereal crop spraying in Tunisian conditions. 10<sup>th</sup> International Congress on Mechanization and Energy in Agriculture, Antalya, Turkey; pp.1-7.
- Cao, X., J. Liua, N. Jiangb and Q. Chena. 2014. Particle image velocimetry measurement of indoor airflow field: A review of the technologies and applications. *Energy Build.* 69: 367-380.
- Dabiri, D. 2009. Digital particle image thermometry/velocimetry: a review. *Exp. Fluids* 46:191-241.
- Grant, I. 1997. Particle image velocimetry: a review. *Proc. Instn. Mech. Engrs.* 211:55-76.
- Guler, H., H. Zhu, H.E. Ozkan, R.C. Derksen, Y. Yu and C.R. Krause. 2007. Spray characteristics and drift reduction potential with air induction and conventional flat-fan nozzles. *Trans. ASABE* 50:745-754.
- Hain, R., C.J. Kahler and C. Tropea. 2007. Comparison of CCD, CMOS and intensified cameras. *Exp. Fluids* 42:403-411.
- Husted, B.P., P. Petersson, I. Lund and G. Holmstedt. 2009. Comparison of PIV and PDA droplet velocity measurement techniques on two high-pressure water mist nozzles. *Fire Saf. J.* 44:1030-1045.
- Marcal, A.R.S. and M. Cunha. 2008. Image processing of artificial targets for automatic evaluation of spray quality. *Trans. ASABE* 51:811-821.
- Miller, P.C.H. and E.M.B. Ellis. 2000. Effects of formulation on spray nozzle performance for applications from ground-based boom sprayers. *Crop Prot.* 19:609-615.
- Morgan, R.G., C.N. Markides, I. Zadrazil and G.F. Hewitt. 2013. Characteristics of horizontal liquid-liquid flows in a circular pipe using simultaneous high-speed laser-induced fluorescence and particle velocimetry. *Int. J. Multiphase Flow* 49:99-118.
- Otsu, N. 1979. A threshold selection method from gray-level histograms. *IEEE Trans. Comput.* 9:62-66.
- Santiago, J.G., S.T. Wereley, C.D. Meinhart, D.J. Beebe and R.J. Adrian. 1998. A particle image velocimetry system for microfluidics. *Exp. Fluids.* 25:316-319.
- Sudheer, P.K. and R.K. Panda. 2000. Digital image processing for determining drop sizes from irrigation spray nozzles. *Agr. Water Manage.* 45:159-167.